Sequence Adaptive Peptide-Polysaccharide Nanostructures by Biocatalytic Self-Assembly

Yousef M. Abul-Haija[‡] *and Rein V. Ulijn*[*,‡,†]

[‡]WestCHEM/Department of Pure & Applied Chemistry and Technology & Innovation Centre, University of Strathclyde, 99 George Street, Glasgow G1 1RD, United Kingdom.

[†]Advanced Science Research Center (ASRC) and Hunter College, City University of New York, 85 St Nicholas Terrace, New York NY 10031, United States.

* Corresponding author:

Rein V. Ulijn

Email: rein.ulijn@asrc.cuny.edu

KEYWORDS

adaptive materials; reconfigurable nanostructures; sequence exchange; biocatalysis; co-assembly; aromatic peptide amphiphiles

ABSTRACT

Co-assembly of peptides and polysaccharides can give rise to formation of nanostructures with tunable morphologies. We show that *in situ* enzymatic exchange of a dipeptide sequences in aromatic peptide amphiphiles/polysaccharide co-assemblies enables dynamic formation and degradation of different nanostructures depending on the nature of the polysaccharide present. This is achieved in a one-pot system composed of Fmoc-cystic acid (CA), Fmoc-lysine (K) plus phenylalanine amide (F) in the presence of thermolysin which, through dynamic hydrolysis and amide formation gives rise to dynamic peptide library composed of the corresponding Fmoc-dipeptides (CAF and KF). When the cationic polysaccharide chitosan is added to this mixture, selective amplification of the CAF peptide is observed giving rise to formation of nanosheets through co-assembly. By contrast, upon addition of anionic heparin, KF is formed which gives rise to a nanotube morphology. The dynamic adaptive potential was demonstrated by sequential morphology changes depending on the sequence of polysaccharide addition. This first demonstration of the ability to access different peptide sequences and nanostructures depending on presence of biopolymers may pave the way to biomaterials that can adapt their structure and function and may be of relevance in design of materials able to undergo dynamic morphogenesis.

INTRODUCTION

Self-assembly[1-3] coupled with biocatalysis[4-6] provides a useful approach for fabrication of adaptive nanostructures, inspired by dynamic processes in living systems. In biology, components interact, assemble, compete and selectively decompose when they are no longer required.[7] To date, few synthetic mimics have focused on dynamic features–which would be key to forming truly adaptive structures. Some examples now exist of reconfigurable materials[8] that

are able to respond to changes in their environment by readjusting their morphology and/or function cooperatively.[2, 9] In addition, selective enzymatic degradation of polymer bioconjugates depending on charge, by taking advantage of electrostatics to enhance or reduce degradation has been described recently.[10] Adaption in terms of changes in molecular composition- achieved through selective and competitive degradation and formation of different compounds to adapt molecular composition to suit certain conditions- has not been described to date in a synthetic system.

A potentially useful approach to achieving molecular adaption of soft biomaterials would involve changing molecular composition through reversible catalytic reactions, using the tools of dynamic combinatorial chemistry (DCC).[11-14] In this approach, building blocks with exchangeable components are formed through reversible interactions to create a dynamic mixture.[15-17] Molecular recognition and assembly between these building blocks (or with externally added templates) then give rise to autonomous optimization of the noncovalent interactions, *i.e.* the most thermodynamically stable product is amplified selectively.[18]

Peptides are particularly useful as building blocks in DCC in a biomaterials context, due to the rich chemistry and functionality available from primary sequences of twenty amino acids, as well as their biological relevance.[19] We have previously developed enzymatically driven peptide libraries that operate through dynamic peptide sequence exchange. It could be demonstrated that the free energy contribution of self-assembly event is sufficient to amplify formation of those peptides that assemble most preferentially at the expense of less potent assembling sequences. Thus, the enzyme driven peptide libraries are useful as tools to identify self-assembling peptide derivatives in a library through continuous formation and hydrolysis of the amide bond.[20,21]

The properties of peptide nanostructures can be altered dramatically by co-assembly[22, 23] with macromolecules where specific interactions (*e.g.* electrostatic, aromatic stacking) and templating[24] might be utilized to direct the assembly process. Recently, Ni and Chau demonstrated the formation of a virus mimic through the electrostatic co-assembly of an oligopeptide with DNA.[25] Stupp and co-workers demonstrated the co-assembly of cationic short peptide amphiphiles and anionic biopolymers (hyaluronic acid, HA), resulting in the formation of hierarchically structured macroscopic sacs and membranes.[26-28] Adams and colleagues reported on the control of mechanical properties of dipeptide derivatives through polymer co-assembly.[29] Mata's group described hybrid multifunctional nanofibrous membranes based on electrostatic interactions between the co-assembled cationic peptide and anionic biopolymer (HA).[30] It is clear from these examples that co-assembly between biopolymers and self-assembling peptides can have dramatic effects on materials properties and consequent function.

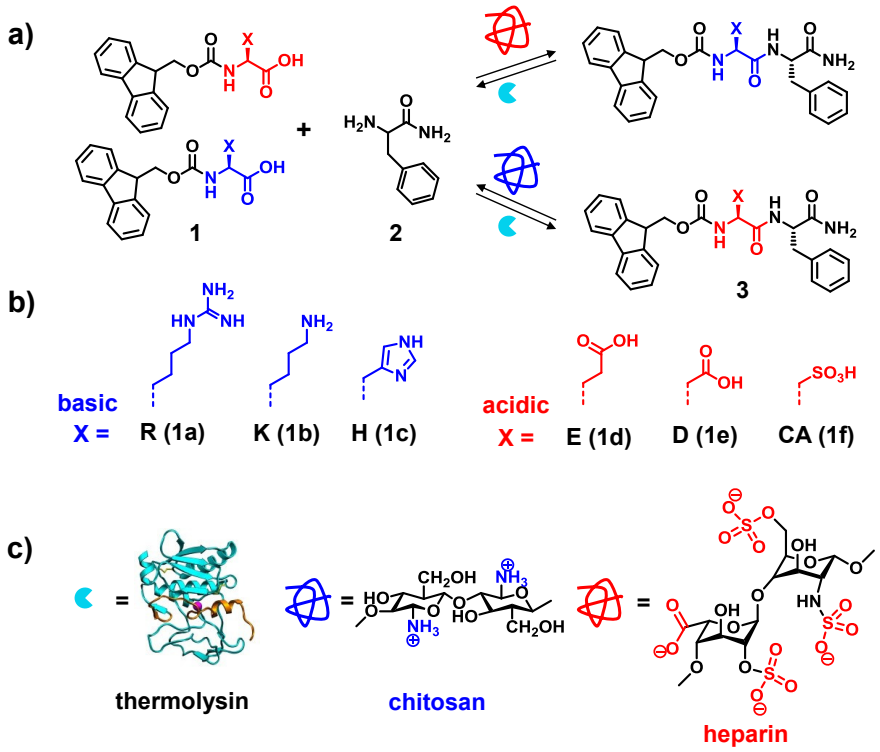

Figure 1. a) Enzymatically triggered *in situ* condensation reaction in which Fmoc-dipeptide derivatives **3** were formed from Fmoc-amino acid **1** (b) (with variable pK_a values on the side chain) and phenylalanine amide **2**. **3** formation and assembly to form nanostructures *via* biocatalytic amide condensation and assembly of the formed Fmoc-peptide amides **3** was evaluated in the presence and absence of biopolymers (c).

Here, we combine these two areas and investigate whether dynamic peptide-polymer assembly can be achieved. Specifically, we show that, by combining dynamic and reversible enzymatic catalyzed peptide sequence exchange (using dynamic peptide libraries) and sequence selective peptide/polymer co-assembly, nanostructures may be developed which change their molecular composition and nanoscale structure depending on the biopolymer present by readjusting molecular composition.

The components of the system are given in **Figure 1**. Systems were designed based on three criteria: (i) peptide components should undergo a fully reversible amide condensation and hydrolysis, but should not give rise to significant self-assembly in the *absence* of the polysaccharide template (*i.e.* low yields of **3** in absence of oppositely charged polymers); (ii) charged Fmoc-dipeptides **3** should be selected and amplified by electrostatic co-assembly between peptide and oppositely charged polysaccharide (with no amplification when the equal charged polymer is added); (iii) it should be possible to reconfigure these systems (to demonstrate peptide sequence adaption) by sequential addition of oppositely charged polymers, demonstrating both amplification and degradation driven by electrostatic co-assembly.

Building on previous enzyme-driven dynamic peptide libraries, we used N-fluorenyl-9-methoxycarbonyl (Fmoc) capped dipeptide amides as a model system to demonstrate the concept (**Figure 1**). These aromatic peptide amphiphiles[31, 32] are known to self-assemble through the combination of π-stacking interactions (among the fluorenyl components) and hydrogen bonding interactions (between the peptides). We previously demonstrated the use of fully reversible enzymatic condensation of Fmoc-amino acid with amino acid esters and amides to produce self-assembling Fmoc-dipeptides. These previous systems used amino acids with uncharged side chains, thereby favoring assembly of the resulting neutral building blocks through a combination of hydrogen bonding between peptide bonds and aromatic interactions between the Fmoc capping groups.[33, 34] In the current work, we focus on introduction of charged amino acids, thus giving low yielding enzymatic condensation as self-assembly of resulting charged Fmoc-peptides is expected to be less favored, unless they can be stabilized by selective co-assembly with charged biopolymers. Furthermore, when these anionic and cationic precursors are combined in one pot, competition between components may produce a sequence adaptive system whereby an

added charged polymer will select (by electrostatic complex formation) the oppositely charged sequence by its selective synthesis while equal charged residues are degraded. Such peptide sequence adaption has not been described before for co-assembled biomaterials. A previous report on sequence adaption details the co-assembly of dynamically coupled short peptides but did not show dynamic formation/degradation and exchange of the peptide bond. [34]

EXPERIMENTAL SECTION

Materials

All chemicals were commercially available and were used without further purification. Fmoc protected (R, K, H, D, CA) and F-NH_2 were purchased from Bachem. Fmoc protected E was purchased from Fluorochem. Thermolysin and chitosan were purchased from Sigma. Heparin sodium salt from porcine intestinal mucosa was purchased from Millipore.

Methods

High-Performance Liquid Chromatography (HPLC).

A Dionex P680 HPLC system was used to quantify conversions of the enzymatic reaction. A 50 µl sample was injected onto a Macherey-Nagel C18 column with a length of 250 mm and an internal diameter of 4.6 mm and 5-mm fused silica particles at a flow rate of 1 $ml.min^{-1}$. The eluting solvent system had a linear gradient of 20% (v/v) acetonitrile in water for 4 min, gradually rising to 80% (v/v) acetonitrile in water at 35 min. This concentration was kept constant until 40 min when the gradient was decreased to 20% (v/v) acetonitrile in water at 42 min. Sample preparation involved mixing 30 µl of sample with acetonitrile–water (1 ml, 70:30

mixture) containing 0.1% trifluoroacetic acid. The purity of each identified peak was determined by UV detection at 280 nm.

Transmission Electron Microscopy (TEM).

Carbon-coated copper grids (200 mesh) were glow discharged in air for 30 s. The grid was touched onto the mixture surface and blotted down using a filter paper. Negative stain (20 µl, 1% aqueous methylamine vanadate obtained from Nanovan; Nanoprobes) was applied and the excess was removed using filter paper. The dried samples were then imaged using a LEO 912 energy filtering TEM operating at 120 kV fitted with 14 bit/2 K Proscan CCD camera.

Atomic Force Microscopy (AFM).

20 µl of the prepared samples was placed on a trimmed and freshly cleaved mica sheet (G250-2 Mica sheets 1" x 1" x 0.006"; Agar Scientific Ltd, Essex, UK) attached to an AFM support stub and left to air-dry overnight in a dust-free environment, prior to imaging. The images were obtained by scanning the mica surface in air under ambient conditions using a Veeco diINNOVA Scanning Probe Microscope (VEECO/BRUKER, Santa Barbara, CA, USA) operated in tapping mode. The AFM scans were taken at 512 x 512 pixels resolution. Typical scanning parameters were as follows: tapping frequency 308 kHz, integral and proportional gains 0.3 and 0.5, respectively, set point 0.5–0.8 V and scanning speed 0.5 Hz. The images were analyzed using NanoScope Analysis software Version 1.40.

Fourier Transform Infrared (FTIR) Spectroscopy.

Spectra were acquired using a Bruker Vertex 70 spectrometer with a spectral resolution of 1 cm^{-1}. The spectra were obtained by averaging 25 scans per sample. Measurements were performed

in a standard IR cuvette (Harrick Scientific), in which the sample was contained between two CaF_2 windows (thickness, 2 mm) separated by a 25 μm PTFE spacer. All sample manipulations were performed in a glove box to minimize interference from atmospheric water vapour. D_2O (Sigma-Aldrich) was used as the solvent for all the infrared spectral measurements. Spectra were recorded after 24 hours of sample preparation.

RESULTS AND DISCUSSION

Our first objective was to identify Fmoc-dipeptides that undergo a fully reversible biocatalytic condensation/hydrolysis but do not give rise to significant self-assembly in the absence of the polysaccharide template. Charged Fmoc-amino acids (*i.e.* +ve: Arginine R (**1a**); Lysine K (**1b**); Histidine H (**1c**) or -ve: Glutamic Acid E (**1d**); Aspartic Acid D (**1e**); Cysteic Acid CA (**1f**)) with different side chain pK_a values (**Table 1**) were incubated individually with four-fold excess (based on previous protocols, see [20, 34]) of phenylalanine-NH_2 (F-NH_2, **2**) at varying concentrations (**Table S1**) in the presence of thermolysin (1 $mg.ml^{-1}$), in 100 mM sodium phosphate buffer pH 7.4 , **Figure 1**.

After enzyme addition, mixtures were vortexed and sonicated to allow dissolution. %yields of products **3a-3f** were evaluated by HPLC after 24 and again at 48 hours (to ensure equilibrium has been reached), **Table 1**. **Table S1** provides the HPLC results obtained for amino acids with basic side chains with varying pK_a values (**1a-1c**) using different concentrations.

Table 1. Yields of *in situ* condensation reaction in the absence and presence of biopolymers (heparin or chitosan) analyzed by HPLC.

entry	pK_a	%Yield		
		None	Heparin	Chitosan
1a	12.48	0	0	0
1b	10.54	9	72	9
1c	6.04	98	98	98
1d	4.07	Excluded; 3 products (Figure S1)		
1e	3.9	92	91	91
1f	1.3	10	9	92

To ultimately produce a system able to dynamically adapt its sequence driven by co-assembly with a charged polymer, we require low yielding amide formation to provide opportunities for electrostatic co-assembly driving the reaction to higher yields. In the absence of biopolymers, **1a** did not form the dipeptide derivative (**3a**) while **3b** was produced in a low yield (9%). **3c** formed in a high yield (98%), in the absence of an external template which is likely due to suppression of the imidazole ionization thus leading to favorable self-assembly of Fmoc-His-Phe-NH_2 (**3c**). Thus, **1b** was judged to be a suitable starting material which could give rise to electrostatic co-assembly induced amplification of its peptide product, **3b**.

For the basic amino acids discussed above, the ratio of 20:80 mM of **1**:**2** gave rise to the most pronounced difference in assembly yield in the absence and presence of polysaccharide. The

concentration of amino acids with acidic side chains (**1d-1f**) was then also fixed at this value (*i.e.* 20:80) for consistency.

Again, anionic amino acids with varying pK_a values were selected. Upon addition of thermolysin to the **1d/2** mixture, **1d** formed three products which included the side chain condensation (through the aspartic acid side chain) and was therefore disregarded (as demonstrated by LC/MS, **Figure S1**). Fmoc-peptide **3e** (the glutamic acid analog) was formed in a high yield (92%), even in absence of the charged polymer, thought to be a result of suppressed ionization of the side chain, therefore enabling assembly of the uncharged **3e**. It was judged that a more acidic amino acid (of lower pK_a) was required to ensure substantial electrostatic repulsion of the free peptide, to prevent substantial assembly in the presence of polymer. Thus, non-canonical Fmoc-cystic acid was selected (**1f**) and it was found that **3f** was formed in a low yield (10%), thus mirroring the results of **1b**/**3b** for the basic Fmoc-amino acid starting material.

From the results of both the basic (**1a-c**) and acidic (**1d-f**), it is clear that the pK_a value has a substantial effect on the condensation reaction where amino acid derivatives with either high or low pK_a values (**1a**, **1b** and **1f**) showed limited yields. In the absence of an oppositely charged polymer, one would expect low levels of assembly of charged Fmoc-dipeptides. As discussed, the formation of **3c** and **3e** in high yields is most likely due to suppression of ionization of the side chains upon self-assembly (as observed previously for terminal carboxylates in self-assembling Fmoc-peptides[35]), giving rise to high yielding nanostructures. Thus, **1b** and **1f** are the best candidates for amplification by peptide/polymer electrostatic co-assembly as their pK_a values prevent their assembly at neutral pH.

The next objective was to show that charged dipeptides can be amplified by electrostatic co-assembly between peptide and oppositely charged polysaccharide, thus shifting the amide condensation/hydrolysis further towards condensation driven by free energy contributions of the electrostatic complexation. We therefore studied the co-assembly effect of oppositely charged biopolymers. For this purpose, polyanionic heparin and polycationic chitosan were selected (**Figure 1**).

Polysaccharide concentrations were calculated on the basis of 1:1 charge equivalents with the charged amino acids used, as follows. Calculations were based on the molecular structure of the polysaccharide repeating units, thus assuming that the entire mass of polymer added is fully composed of these repeats (these calculations are based on previous reports.[36, 37] Chitosan is composed of two types of repeating units, glucosamine (Mw = 161) and N-acetyl-glucosamine (Mw = 203). The degree of deacetylation of the chitosan was 75%; therefore, the average molecular weight of the repeating unit is 171.5. This approach was described previously.[36] Heparin was obtained as the sodiated analogue structure shown in **Figure 1c**, with molecular weight of 665.4 $g.mol^{-1}$ and 4 negative charges per repeating unit.[37]

Chitosan was dissolved in 0.5% acetic acid first then added with the pH value adjusted to 7.4 with 0.5 M HCl/NaOH as required. Gratifyingly, enzymatic condensation yields were increased substantially in the presence of the oppositely charged biopolymer to 72% for **3b** in the presence of heparin while chitosan did not impact on the condensation yield. For **3f**, an amplification to 92% was observed in the presence of chitosan, while the yield was unaffected by heparin. Thus, these results clearly show selection of the oppositely charged peptide by electrostatic templating of the condensation product. As expected, yields were not significantly affected in the case of

1/3a (no condensation observed**)**, **1/3c** and **1/3e** (high yield observed regardless of presence of polymer). Therefore, only **1b** and **1f** were considered further in this study.

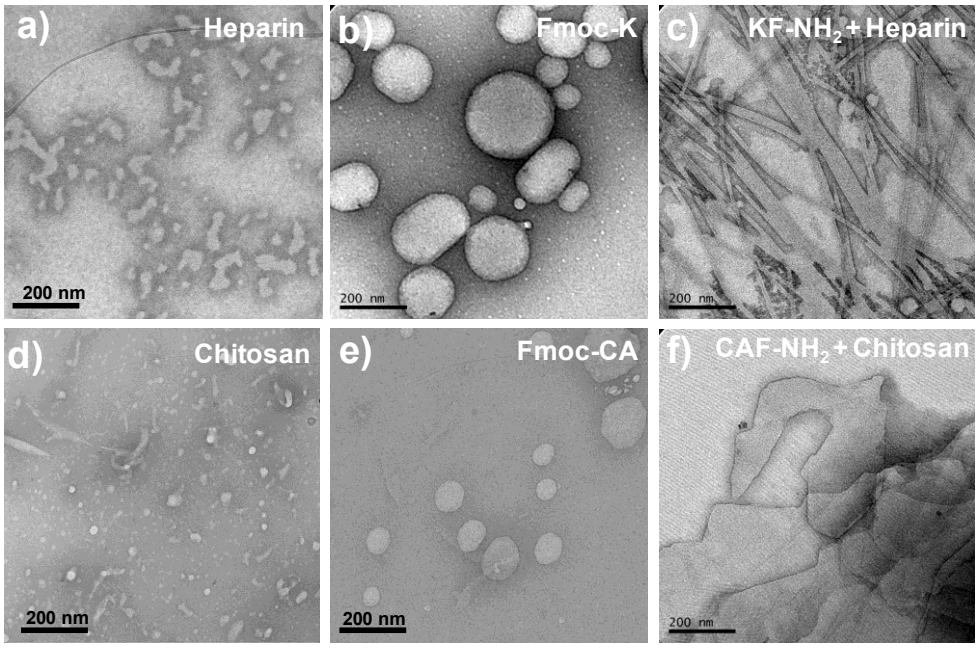

Figure 2. TEM images showing random aggregates of biopolymers (a,d) and spherical aggregates of precursors (**1b** and **1f**/ b, e) and differential co-assembly into nanotubes and nanosheets depending on the nature of the biopolymer present (c, f). Scale bar = 200 nm.

Next, we investigated whether the **3b** and **3f** co-assembled systems display differential co-assembly and express different morphologies depending on composition. To gain insights into the morphology of the co-assembled nanostructures formed, precursors and products of selected candidates were examined by transmission electron microscope (TEM), **Figure 2**. TEM images show random aggregates of biopolymers, spherical aggregates of precursors (**1b** and **1f**) and differential co-assembly leading to the formation of **3b** nanotubes (morphologically similar to previously reported examples[38]) and **3f** nanoscale sheets depending on complimentary biopolymer (additional TEM and AFM images are included in **Figure S3-S5** in the SI).

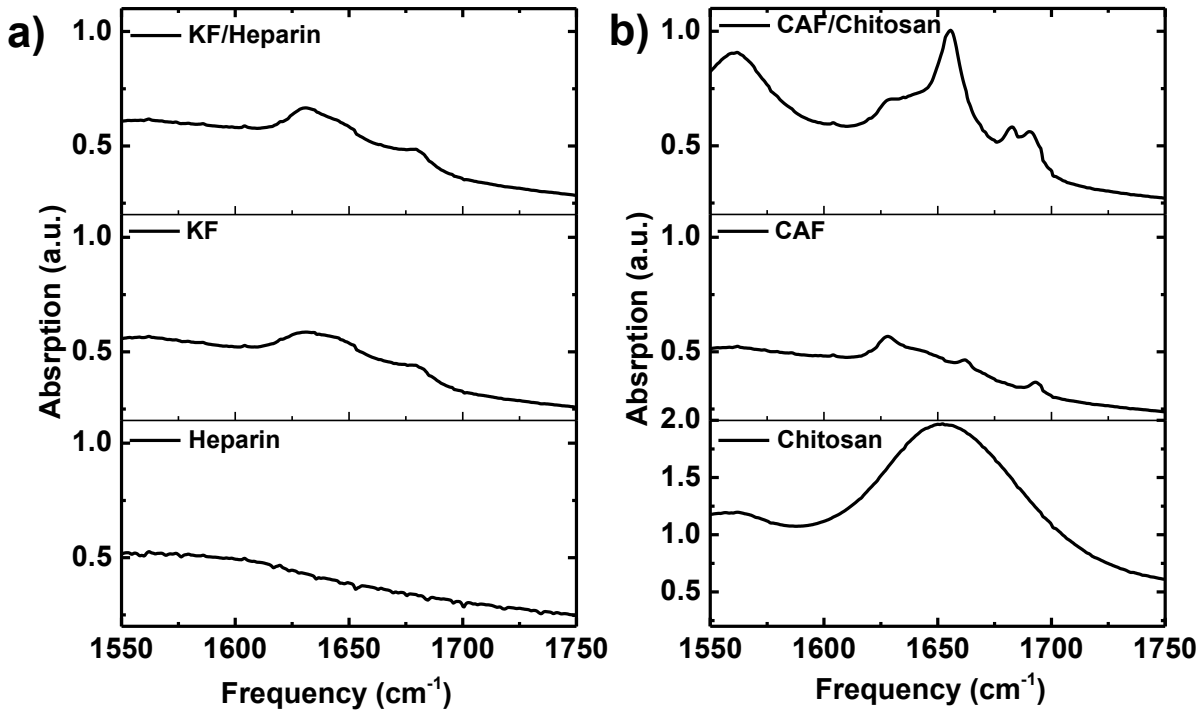

Figure 3. Infrared absorption spectra for Fmoc-dipeptides (**3b**, left and **3f**, right) assembled in absence and presence of polysaccharides with opposite charges (heparin and chitosan).

In order to study H-bonding interactions in Fmoc-peptide assembly, FTIR measurements were performed for Fmoc-dipeptides before and after polysaccharides addition (**Figure 3**). Self-assembled Fmoc dipeptides are known to show two main IR absorption peaks (at around 1630 cm^{-1} and 1680 cm^{-1}) which are characteristic for β-sheet like interactions and carbamate stacking, respectively.[39] Before heparin addition, KF showed peaks at 1634 cm^{-1} and 1681 cm^{-1}. After adding heparin to the dipeptide both peaks increased in intensity with the former peak shifted to a lower frequency (1630 cm^{-1}). These observations suggest a stronger H-bonding and a higher molecular organization upon co-assembly. Similarly, CAF spectrum showed peaks at 1628 cm^{-1} and 1693 cm^{-1} before adding chitosan, which increased in intensity after the polysaccharide addition. An extra peak at 1662 cm^{-1} suggests the presence of unstructured (less organized)

peptide as previously reported.[40] After interacting with chitosan, the spectrum showed a peak at 1683 cm^{-1}, which suggests a different type of interactions in its presence. CAF/Chitosan spectrum showed extra peaks at 1561 cm^{-1} and 1655 cm^{-1} which are characteristic peaks for the C=O bonds vibrational bands of chitosan[41]; the protonated amino group (or salt-bridged group) and CONHR amide group (chitosan's degree of deacetylation is 75%).

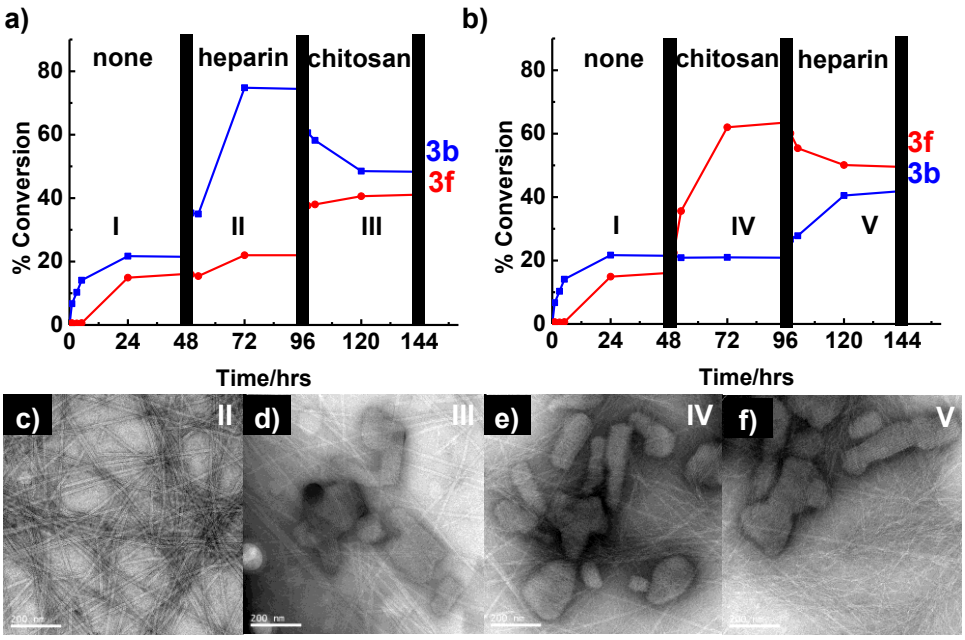

Figure 4. (a-b) HPLC data showing % conversion for a) **1b**, **1f**, **2** and thermolysin at 48 hours (Stage I) followed by addition of heparin (Stage II) followed by addition of chitosan (Stage III). b) Stage I was followed by addition of chitosan (Stage IV) followed by heparin (Stage V). (c-f) TEM images of nanostructures formed. c) Nanotubes dominating after Stage II. d) Nanosheets were mainly formed after Stage III in addition to tubes/fibers. e) Nanotubes and nanosheets formed after Stage IV. f) A mixture of nanostructures was formed after Stage V. Scale bar = 200 nm.

Having established a system that shows sequence-selective amplification driven by electrostatic peptide/polymer co-assembly, we then tested the adaptive potential of a mixed system that could

express different morphologies, depending on the polymer added. Thus, selected components (*i.e.* **1b**, **1f**, **2** and thermolysin) were mixed in one pot and allowed to react during 48 hours to make sure that the system reached equilibrium (**Figure 4/a-b**). Low yield (21% and 16%) was produced for **3b** and **3f** respectively. These yields were higher compared to those observed when either **1b** or **1f** were present in isolation, showing that having both charged species **1b** and **1f** present simultaneously increases the yields, most likely through co-assembly of the charge complementary peptides **3b** and **3f**.[42] To investigate this further, FTIR measurements were performed for **3b/3f** co-assembled mixture. Compared to **3b** and **3f** spectra in isolation (**Figure 3**), the spectrum in **Figure S6** shows main peaks; at 1631 cm^{-1}, 1680 cm^{-1} and 1692 cm^{-1}, with a sharper peak at 1631 cm^{-1} which might suggest co-assembly between **3b** and **3f**. As discussed, polysaccharides stabilize oppositely charged assemblies which lead to a shift in equilibrium towards these products. So, heparin biopolymer was added to the mixture forming **3b** selectively (74% after 48 hours). The selective formation of **3b** was attributed to the electrostatic interaction of positively charged **3b** and polyanionic heparin. Then, chitosan was added to the same mixture which led for **3b** hydrolyze while **3f** was amplified. At 144 hours, **3b** formed at 48% and **3f** 41%. Similarly, adding polycationic chitosan to the amino acids mixture selectively forms **3f** (63% after 48 hours). Adding heparin to the same mixture led to decomposition of part of **3f** (49%) and formation of **3b** at 42%. This clearly shows that the designed system is dynamic and adaptive as it can exchange peptide sequence through competition and selectively decomposition driven by electrostatic templating effect of biopolymers present. It should be noted that the final compositions in each case are similar, but not identical showing that full thermodynamic control is not achieved. This is likely to formation of kinetically trapped aggregates that are not easily accessible by the biocatalyst.

The morphology change of amino acid/dipeptide derivatives was evaluated using TEM, **Figure 4/c-f**. Before the enzyme addition, amino acid derivatives formed spherical aggregates (**Figure S2a**). After the addition of enzyme and after 48 hours, few nanotubes and nanosheets of **3b** and **3f** respectively were observed (**Figure S2b**). Adding heparin selectively enhances the formation of **3b** nanotubes (**Figure 4c**) while the addition of chitosan amplifies the formation of **3f** nanosheets (**Figure 4d**), while some tubes/fibers can also be observed. **Figure 4e** shows the formation of nanosheets and fibers during initial co-assembly with chitosan, the fibers observed here were not present in the absence of Fmoc-KF-NH_2 (**Figure 2f**) suggesting these fibers may represent Fmoc-KF-NH_2 or a degree of co-assembly between the Fmoc-K/CA dipetides. **Figure 4f** resembles **Figure 4d**, where both types of nanostructures are clearly observed, in agreement with approximately equal concentrations of **3b** and **3f**.

CONCLUSIONS

In summary, we successfully demonstrated adaptive biocatalytic co-assembly through the combination of enzymatically triggered *in situ* condensation reaction, dynamic combinatorial chemistry and co-assembly with biopolymers holding opposite charge (which acted as templates). Amide bond formation could be enhanced substantially due to the template presence (*i.e.* electrostatic interactions between amino acids and biopolymer macromolecules), which in turn led to form reconfigurable structures; from spherical aggregates to nanotubes or nanosheets depending on the template. Overall, these adaptive biomaterials display sequence and structure adaption by competing catalytic amplification and decomposition giving rise to morphological adaption under constant conditions. The mechanism of amplification by electrostatic co-assembly is likely not exclusive to saccharides. Indeed, significant cooperative effects have been observed in co-assembly of Fmoc-peptides with (charged) proteins[23] and it will be interesting to

investigate the possibility of adaptive reconfiguration in response to protein templating. More generally, we expect the methodology developed here to be of relevance in development of synthetic morphogenesis, by inclusion of non-equilibrium catalytic assembly[43] to transient co-assembled structures.

Supporting Information.

Experimental details, additional HPLC, LC/MS results and TEM images. This material is available free of charge via the Internet at http://pubs.acs.org.

Corresponding Author

*Rein V. Ulijn

Email: rein.ulijn@asrc.cuny.edu

ACKNOWLEDGMENT

We acknowledge financial support from the European Research Council *via* the initial training network ReAd (Contract No. 289723) and (FP7/2007-2013)/EMERgE/ERC Grant Agreement No. (258775). We would like also to thank Gary Scott, Ivan Sasselli and Neil Hunt for their help with FTIR spectroscopy.

REFERENCES

1. Whitesides, G. M.; Grzybowski, B., Self-Assembly at All Scales. *Science* **2002,** 295, (5564), 2418-2421.
2. Aida, T.; Meijer, E.; Stupp, S., Functional supramolecular polymers. *Science* **2012,** 335, (6070), 813-817.
3. Lehn, J.-M., Perspectives in Chemistry—Aspects of Adaptive Chemistry and Materials. *Angew. Chem. Int. Ed.* **2015,** 54, (11), 3276-3289.
4. Yang, Z.; Gu, H.; Fu, D.; Gao, P.; Lam, J. K.; Xu, B., Enzymatic Formation of Supramolecular Hydrogels. *Adv. Mater.* **2004,** 16, (16), 1440-1444.

5. Zhou, J.; Du, X.; Gao, Y.; Shi, J.; Xu, B., Aromatic–Aromatic Interactions Enhance Interfiber Contacts for Enzymatic Formation of a Spontaneously Aligned Supramolecular Hydrogel. *J. Am. Chem. Soc.* **2014,** 136, (8), 2970-2973.
6. Ku, T.-H.; Sahu, S.; Kosa, N. M.; Pham, K. M.; Burkart, M. D.; Gianneschi, N. C., Tapping a Bacterial Enzymatic Pathway for the Preparation and Manipulation of Synthetic Nanomaterials. *J. Am. Chem. Soc.* **2014,** 136, (50), 17378-17381.
7. Desai, A.; Mitchison, T. J., MICROTUBULE POLYMERIZATION DYNAMICS. *Annu. Rev. Cell Dev. Biol.* **1997,** 13, (1), 83-117.
8. Wang, Y.; Huang, Z.; Kim, Y.; He, Y.; Lee, M., Guest-Driven Inflation of Self-Assembled Nanofibers through Hollow Channel Formation. *J. Am. Chem. Soc.* **2014,** 136, (46), 16152-16155.
9. Badjić, J. D.; Nelson, A.; Cantrill, S. J.; Turnbull, W. B.; Stoddart, J. F., Multivalency and Cooperativity in Supramolecular Chemistry. *Acc. Chem. Res.* **2005,** 38, (9), 723-732.
10. Samarajeewa, S.; Zentay, R. P.; Jhurry, N. D.; Li, A.; Seetho, K.; Zou, J.; Wooley, K. L., Programmed hydrolysis of nanoassemblies by electrostatic interaction-mediated enzymatic-degradation. *Chem. Commun.* **2014,** 50, (8), 968-970.
11. Lehn, J.-M.; Eliseev, A. V., Dynamic Combinatorial Chemistry. *Science* **2001,** 291, (5512), 2331-2332.
12. Otto, S.; Furlan, R. L. E.; Sanders, J. K. M., Dynamic combinatorial chemistry. *Drug Discovery Today* **2002,** 7, (2), 117-125.
13. Maiti, S.; Prins, L. J., Dynamic combinatorial chemistry on a monolayer protected gold nanoparticle. *Chem. Commun.* **2015,** 51, (26), 5714-5716.
14. Li, J.; Nowak, P.; Otto, S., Dynamic Combinatorial Libraries: From Exploring Molecular Recognition to Systems Chemistry. *J. Am. Chem. Soc.* **2013,** 135, (25), 9222-9239.
15. Ruff, Y.; Garavini, V.; Giuseppone, N., Reversible Native Chemical Ligation: A Facile Access to Dynamic Covalent Peptides. *J. Am. Chem. Soc.* **2014,** 136, (17), 6333-6339.
16. Janeliunas, D.; van Rijn, P.; Boekhoven, J.; Minkenberg, C. B.; van Esch, J. H.; Eelkema, R., Aggregation-Driven Reversible Formation of Conjugated Polymers in Water. *Angew. Chem. Int. Ed.* **2013,** 52, (7), 1998-2001.
17. Kang, Y.; Liu, K.; Zhang, X., Supra-Amphiphiles: A New Bridge Between Colloidal Science and Supramolecular Chemistry. *Langmuir* **2014,** 30, (21), 5989-6001.
18. Mattia, E.; Otto, S., Supramolecular systems chemistry. *Nat. Nanotechnol.* **2015,** 10, (2), 111-119.
19. Abul-Haija, Y. M.; Ulijn, R. V., Chapter 6 Enzyme-Responsive Hydrogels for Biomedical Applications. In *Hydrogels in Cell-Based Therapies*, The Royal Society of Chemistry: 2014; pp 112-134.
20. Williams, R. J.; Smith, A. M.; Collins, R.; Hodson, N.; Das, A. K.; Ulijn, R. V., Enzyme-assisted self-assembly under thermodynamic control. *Nat. Nanotechnol.* **2008,** 4, (1), 19-24.
21. Nalluri, S. K. M.; Ulijn, R. V., Discovery of energy transfer nanostructures using gelation-driven dynamic combinatorial libraries. *Chem. Sci.* **2013,** 4, (9), 3699-3705.
22. Cornwell, D. J.; Smith, D. K., Expanding the scope of gels - combining polymers with low-molecular-weight gelators to yield modified self-assembling smart materials with high-tech applications. *Materials Horizons* **2015,** 2, (3), 279-293.
23. Chen, L.; Revel, S.; Morris, K.; Spiller, D. G.; Serpell, L. C.; Adams, D. J., Low molecular weight gelator-dextran composites. *Chem. Commun.* **2010,** 46, (36), 6738-6740.

24. Javid, N.; Roy, S.; Zelzer, M.; Yang, Z.; Sefcik, J.; Ulijn, R. V., Cooperative Self-Assembly of Peptide Gelators and Proteins. *Biomacromolecules* **2013,** 14, (12), 4368-4376.
25. Ni, R.; Chau, Y., Structural Mimics of Viruses Through Peptide/DNA Co-Assembly. *J. Am. Chem. Soc.* **2014,** 136, (52), 17902-17905.
26. Carvajal, D.; Bitton, R.; Mantei, J. R.; Velichko, Y. S.; Stupp, S. I.; Shull, K. R., Physical properties of hierarchically ordered self-assembled planar and spherical membranes. *Soft Matter* **2010,** 6, (8), 1816-1823.
27. Capito, R. M.; Azevedo, H. S.; Velichko, Y. S.; Mata, A.; Stupp, S. I., Self-Assembly of Large and Small Molecules into Hierarchically Ordered Sacs and Membranes. *Science* **2008,** 319, (5871), 1812-1816.
28. Chow, L. W.; Bitton, R.; Webber, M. J.; Carvajal, D.; Shull, K. R.; Sharma, A. K.; Stupp, S. I., A bioactive self-assembled membrane to promote angiogenesis. *Biomaterials* **2011,** 32, (6), 1574-1582.
29. Pont, G.; Chen, L.; Spiller, D. G.; Adams, D. J., The effect of polymer additives on the rheological properties of dipeptide hydrogelators. *Soft Matter* **2012,** 8, (30), 7797-7802.
30. Mendes, A. C.; Smith, K. H.; Tejeda-Montes, E.; Engel, E.; Reis, R. L.; Azevedo, H. S.; Mata, A., Co-Assembled and Microfabricated Bioactive Membranes. *Adv. Funct. Mater.* **2013,** 23, (4), 430-438.
31. Fleming, S.; Ulijn, R. V., Design of nanostructures based on aromatic peptide amphiphiles. *Chem. Soc. Rev.* **2014,** 43, (23), 8150-8177.
32. Zhang, Y.; Gu, H.; Yang, Z.; Xu, B., Supramolecular hydrogels respond to ligand-receptor interaction. *J. Am. Chem. Soc.* **2003,** 125, (45), 13680-13681.
33. Pappas, C. G.; Abul-Haija, Y. M.; Flack, A.; Frederix, P. W. J. M.; Ulijn, R. V., Tuneable Fmoc-Phe-(4-X)-Phe-NH2 nanostructures by variable electronic substitution. *Chem. Commun.* **2014,** 50, (73), 10630-10633.
34. Toledano, S.; Williams, R. J.; Jayawarna, V.; Ulijn, R. V., Enzyme-triggered self-assembly of peptide hydrogels via reversed hydrolysis. *J. Am. Chem. Soc.* **2006,** 128, (4), 1070-1071.
35. Tang, C.; Smith, A. M.; Collins, R. F.; Ulijn, R. V.; Saiani, A., Fmoc-Diphenylalanine Self-Assembly Mechanism Induces Apparent p K a Shifts. *Langmuir* **2009,** 25, (16), 9447-9453.
36. Tsai, S.-P.; Hsieh, C.-Y.; Hsieh, C.-Y.; Wang, D.-M.; Huang, L. L.-H.; Lai, J.-Y.; Hsieh, H.-J., Preparation and cell compatibility evaluation of chitosan/collagen composite scaffolds using amino acids as crosslinking bridges. *J. Appl. Polym. Sci.* **2007,** 105, (4), 1774-1785.
37. Bromfield, S. M.; Barnard, A.; Posocco, P.; Fermeglia, M.; Pricl, S.; Smith, D. K., Mallard Blue: A High-Affinity Selective Heparin Sensor That Operates in Highly Competitive Media. *J. Am. Chem. Soc.* **2013,** 135, (8), 2911-2914.
38. Xu, H.; Das, A. K.; Horie, M.; Shaik, M. S.; Smith, A. M.; Luo, Y.; Lu, X.; Collins, R.; Liem, S. Y.; Song, A.; Popelier, P. L. A.; Turner, M. L.; Xiao, P.; Kinloch, I. A.; Ulijn, R. V., An investigation of the conductivity of peptide nanotube networks prepared by enzyme-triggered self-assembly. *Nanoscale* **2010,** 2, (6), 960-966.
39. Fleming, S.; Debnath, S.; Frederix, P. W. J. M.; Tuttle, T.; Ulijn, R. V., Aromatic peptide amphiphiles: significance of the Fmoc moiety. *Chem. Commun.* **2013,** 49, (90), 10587-10589.
40. Barth, A.; Zscherp, C., What vibrations tell about proteins. *Q. Rev. Biophys.* **2002,** 35, (04), 369-430.
41. García, M. A.; de la Paz, N.; Castro, C.; Rodríguez, J. L.; Rapado, M.; Zuluaga, R.; Gañán, P.; Casariego, A., Effect of molecular weight reduction by gamma irradiation on the

antioxidant capacity of chitosan from lobster shells. *J. Radiat. Res. Appl. Sci.* **2015,** 8, (2), 190-200.
42. Adhikari, B.; Nanda, J.; Banerjee, A., Multicomponent hydrogels from enantiomeric amino acid derivatives: helical nanofibers, handedness and self-sorting. *Soft Matter* **2011,** 7, (19), 8913-8922.
43. Pappas, C. G.; Sasselli, I. R.; Ulijn, R. V., Biocatalytic Pathway Selection in Transient Tripeptide Nanostructures. *Angew. Chem. Int. Ed.* **2015,** 54, (28), 8119-8123.

TOC Graphic